FPST TOC

Proceedings of IMECE'03
2003 ASME International Mechanical Engineering Congress
Washington, D.C., November 15–21, 2003

IMECE2003-42668

COORDINATE CONTROL OF ENERGY-SAVING PROGRAMMABLE VALVES

Song Liu
Ray. W. Herrick Laboratories
School of Mechanical Engineering
Purdue University
W. Lafayette, IN 47907
Tel: 765-496-6008, Fax: 765-494-0539
Email: liu1@purdue.edu

Bin Yao*
Ray. W. Herrick Laboratories
School of Mechanical Engineering
Purdue University
W. Lafayette, IN 47907
Tel: 765-494-7746, Fax: 765-494-0539
Email: byao@purdue.edu

ABSTRACT

The energy-saving programmable valve, a unique combination of five independent cartridge valves, not only decouples the control of meter-in and meter-out flows but also provides the ability of precisely controlling cross-port flows for energy-saving purpose. Our previous works have already shown that the tremendous control flexibility gained by the proposed hardware re-configuration enables one not only to achieve precision control of the cylinder motion but also to decrease the energy usage significantly through actively utilizing the potential and kinetic energy of the load in accomplishing certain tasks such as smooth stopping. However, the control of such an essentially multi-input valve system to achieve the above objectives is far from trivial. In our previous works, a constant off-side pressure was assumed in the controller design for simplicity. This assumption may not be realistic in certain circumstances where the off-side pressure may vary from the assumed constant pressure significantly, especially right after the change of working mode. As a result, though the controller design is simplified, larger tracking error results during the transients.

This paper presents an improved way to coordinately control the five independent valves by incorporating the off-side pressure dynamics into the controller design. The Adaptive Robust Control technique is applied to guarantee the stability and tracking performance in the presence of large system parameter variations and disturbances. Simulation and experimental results are shown to verify the much improved control performance of the presented coordinate control strategy.

INTRODUCTION

The advent of electro-hydraulic valves and the incorporation of complex digital control have significantly improved the performance of hydraulic systems. A new problem arises as the applications of electro-hydraulic systems becoming increasingly widespread: is it possible to reduce the energy usage while keep the desired performance?

Hydraulic energy used for a certain task can be defined as:

$$E = \int_{t_0}^{t_1} P_s(\tau) Q_s(\tau) d\tau \tag{1}$$

where E represents the hydraulic energy used for a certain task from t_0 to t_1, P_s the hydraulic supply pressure and Q_s the pump flow rate. For a specific task, i.e., t_0 and t_1 are fixed, reducing the energy usage is equivalent to reducing the power (the integrand). Therefore, the word energy is abused for both energy and power though out the paper. It is obvious that there may be two ways to reduce the energy usage:

1. *reduce the supply pressure*
2. *reduce the pump flow rate*

*Address all correspondence to this author.

Copyright © 2003 by ASME

Neglecting the fluid compressibility, the pump flow rate depends only on the task unless regeneration flow is used. To reduce the supply pressure, pressures at the two cylinder chambers are desired to be as low as possible while certain pressure difference is kept to maintain the motion task. Therefore, independent control of two chamber pressures and use of regeneration flow are the key point for energy saving.

Traditionally, a typical four-way directional control valve or servo valve is used to control the hydraulic cylinder as done in almost all existing publications [1–6]. With a such a configuration only one of the two cylinder states, (i.e., pressures of the two chambers), is completely controllable and there is a one-dimensional internal dynamics. Although the one-dimensional internal dynamics is shown to be stable [7], it cannot be modified by any control strategy. The control input is uniquely determined once the desired motion is specified, which makes the regulation of individual cylinder chamber pressures impossible for energy-saving. The result is that while high performance tracking can be attained, simultaneous high levels of energy saving cannot. The uncontrollable state is due to the fact that the meter-in and meter-out orifices are mechanically linked together in a typical directional control valve. This is a fundamental drawback of typical four-way directional control valves. If this link were to be broken, the flexibility of the valve could be drastically increased, making the way for significant improvements in hydraulic efficiency [8].

The technique of breaking the mechanical linkage between the meter-in and meter-out orifices is well known and has been used in heavy industrial applications for several years. Typically, the spool valve is replaced by four poppet type valves [8]. There is a number of slight variations on this theme throughout the mobile hydraulics industry. Patents by Deere & Company, Moline, IL as well as Caterpillar Inc., Joliet, IL. and Moog Inc., East Aurora, NY attest to the potential of this technique [9, 10].

The valve configuration used in this study takes the four-valve poppet type valve [11, 12] and makes the addition of an additional valve to enable true cross port flow. The configuration allows independent meter-in, meter-out control in addition to the availability of cross port regenerative flow. The result is a programmable valve capable of controlling each cylinder state as well as providing regeneration flow for optimal energy usage. The programmable valve configuration used in this study is seen in Fig. 1.

The use of the programmable valve provides multiple inputs to control the two cylinder states. The effect is that both cylinder states, P_1 and P_2, become completely controllable. However, the control of such an essentially multi-input nonlinear system to achieve the dual objectives is far from trivial. The difficulties come not only from the highly nonlinear hydraulic dynamics, large parameter variantions [13], significant uncertain nonlinearities such as external disturbances, flow leakage and seal frictions [1, 5], but also from the coordination of five cartridge

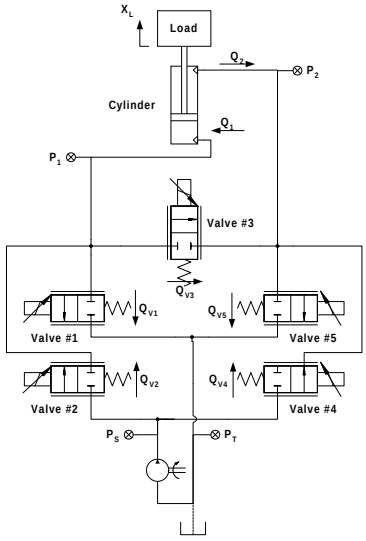

Figure 1. PROGRAMMABLE VALVE LAYOUT.

valves. In our previous works, a constant off-side pressure was assumed in the controller design for simplicity. This assumption may not be realistic in certain circumstances where the off-side pressure may variate from the assumed constant pressure significantly, especially right after the change of working mode. As a result, though the controller design is simplified, larger tracking error results during the transients.

This paper focuses on the coordinate control of the programmable valves. Instead of assuming constant pressure at off-side, the off-side pressure dynamics is considered in the motion controller design. The Adaptive Robust Control technique is applied to guarantee the stability and tracking performance in the presence of large system parameter variations and disturbances.

DYNAMIC MODEL AND PROBLEM FORMULATION

To illustrate the uniqueness and the application of the proposed programmable valves, the boom motion control of a three degree-of-freedom (DOF) electro-hydraulic robot arm that was built to mimic the industrial backhoe or excavator arms in [5] is considered. With the coordinate systems, joint angles and physical parameters of the system defined in Fig. 2, the boom motion

Copyright © 2003 by ASME

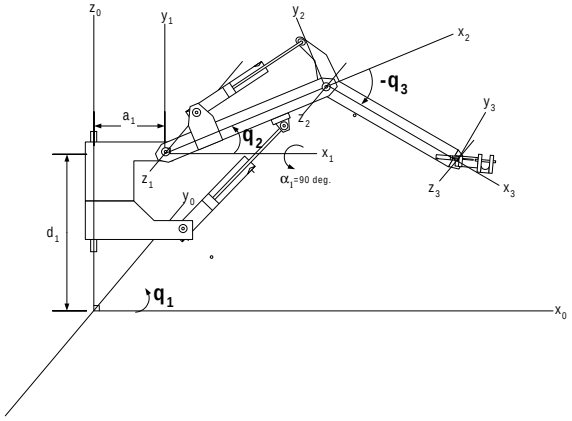

Figure 2. THREE DOF ELECTRO-HYDRAULIC ROBOT ARM.

dynamics with other two joints fixed can be described by [6, 14].

$$(J_c + m_L \ell_e{}^2)\ddot{q_2} = \frac{\partial x_L}{\partial q_2}(P_1 A_1 - P_2 A_2) - G_c(q_2) \\ -m_L g \ell_g(q_2) - D_f \cdot \dot{q} + T(t, q_2, \dot{(q)}_2) \qquad (2)$$

where q_2 represents the boom joint angle, J_c is the moment of inertia of the boom without payload, m_L represents the mass of the unknown payload, G_c is the gravitational load of the boom without payload, x_L represents the boom hydraulic cylinder displacement, P_1 and P_2 are the head and rod end pressures of the cylinder respectively, A_1 and A_2 are the head and rod end areas of the cylinder respectively, D_f is the damping and viscous friction coefficient and T represents the lumped disturbance torque including external disturbances and terms like the unmodelled friction torque. The specific forms of J_c, G_c, ℓ_g, and ℓ_e are given in [6]. The inertial moment and the gravity force both depend on the unknown element m_L. As a result, the inertial moment and the gravity force are split into two components. The terms J_c and $G_c(q_2)$ contain only calculable quantities and the terms $m_L g l_g(q_2)$ and $m_L l_e^2$ which contain the unknown quantity m_L. The unknown terms have to be estimated later on-line via parameter adaptation.

Neglecting cylinder flow leakages, the hydraulic cylinder equations can be written as [1],

$$\frac{V_1(x_L)}{\beta_e}\dot{P_1} = -A_1\dot{x_L} + Q_1 = -A_1\frac{\partial x_L}{\partial q_2}\dot{q_2} + Q_1 \\ \frac{V_2(x_L)}{\beta_e}\dot{P_2} = A_2\dot{x_L} - Q_2 = A_2\frac{\partial x_L}{\partial q_2}\dot{q_2} - Q_2 \qquad (3)$$

where $V_1(x_L) = V_{h1} + A_1 x_L$ and $V_2(x_L) = V_{h2} - A_2 x_L$ are the total cylinder volumes of the head and rod ends including connecting hose volumes respectively, V_{h1} and V_{h2} are the initial control volumes when $x_L = 0$, β_e is the effective bulk modulus. Q_1 and Q_2 are the supply and return flows respectively.

When the programmable valve in Fig.1 is used, Q_1 and Q_2 are given by,

$$Q_1 = Q_{v2} - Q_{v1} - Q_{v3} \\ Q_2 = -Q_{v3} - Q_{v4} + Q_{v5} \qquad (4)$$

where the orifice flows Q_{vi} can be described by

$$Q_{vi} = f_{vi}(\Delta P_{vi}, x_{vi}), \quad i = 1, 2, ...5 \qquad (5)$$

in which f_{vi} is the nonlinear orifice flow mapping as a function of the pressure drop ΔP_{vi}, and the virtual orifice opening x_{vi} of the *ith* cartridge valve. x_{vi} is related to the valve command voltage v_i by an seconde order dynamic approximation (6).

$$\frac{x_{vi}(s)}{v_i(s)} = \frac{\omega_v^2}{s^2 + 2\zeta_v\omega_v s + \omega_v^2} \qquad (6)$$

where the nominal values of natural frequency ω_v and the damping ratio ζ_v are $353.6 rad/sec$ and 1.03 respectively, according to the manufacture's data sheet. The valve dynamics are neglected in controller design due to their sufficiently high bandwidth, but are considered in the system model for simulation.

Due to the fact that the nonlinear flow mappings are very difficult to determine accurately, it is assumed that

$$Q_1 = Q_{1M} + \tilde{Q}_1 \\ Q_2 = Q_{2M} + \tilde{Q}_2 \qquad (7)$$

where Q_{1M} and Q_{2M} represent the flows obtained from the approximated valve mappings and $\tilde{Q}_1$ and $\tilde{Q}_2$ represent the modelling errors of the flow mappings. The effect of the flow modelling errors will be dealt with through robust feedback.

Given the desired motion trajectory $q_{2d}(t)$, the primary objective is to synthesize control voltages for the five cartridge valves such that the output q_2 tracks $q_{2d}(t)$ as closely as possible in spite of various model uncertainties. The second objective is to minimize the overall energy usage.

WORKING MODE SELECTION

The difficulties in the coordinate control of five cartridge valves for precision motion and pressure control are dealt with through a task level and valve level controllers. Given the current working condition, the task level controller determines the

Copyright © 2003 by ASME

Table 1. Programmable valves tracking mode selection

$\dot{x}_d$	P_{lda}	Valve Configuration	Off-side	Mode
>0	>0	$Q_1 = Q_{v2}$ $Q_2 = Q_{v5}$	P_2	T1
>0	<0	$Q_1 = Q_{v2} - Q_{v3}$ $Q_2 = -Q_{v3}$	P_1	T2
<0	>0 $P_1 > P_2$	$Q_1 = -Q_{v3}$ $Q_2 = -Q_{v3} + Q_{v5}$	P_2	T3
<0	>0 $P_1 \leq P2$	$Q_1 = -Q_{v1}$ $Q_2 = -Q_{v4}$	P_2	T4
<0	<0	$Q_1 = -Q_{v1}$ $Q_2 = -Q_{v4}$	P_1	T5

Table 2. Programmable valves regulation mode selection

$\dot{x}_d$	$x - x_d$	Valve Configuration	Off-side	Mode
$=0$	$>\varepsilon$	$Q_1 = -Q_{v3}$ $Q_2 = -Q_{v3} + Q_{v5}$	P_2	R1
$=0$	$<-\varepsilon$	$Q_1 = Q_{v2}$ $Q_2 = Q_{v5}$	P_2	R2
$=0$	*otherwise*	$Q_1 = 0$ $Q_2 = 0$		R3

configurations of programmable valves that would enable significant energy saving while without losing hydraulic circuit controllability for motion tracking, which is sometimes referred to as the working mode selection in hydraulic industry. The valve level controller uses an adaptive robust control technique to control the pressures in both chambers independently with selected working mode to obtain the dual objectives. The working mode selection is introduced in this section and the Adaptive Robust Controller designs are detailed in the following sections.

The task level of the controller determines how the five valves of the proposed programmable valves in Fig. 1 should be used in order to provide the required control flows for motion tracking while maintaining the lowest possible cylinder chamber pressures to reduce the flow losses for energy saving. Obviously, such a process is not unique due to the added flexibility of independently controlling each of these five valves. The working mode selection is task dependent. There are five tracking modes and three regulation modes. The tracking mode selection [14], shown in Table 1, is based on the desired cylinder velocity $\dot{x}_d$, chamber pressures P_1 and P_2 and desired load pressure P_{lda}, which would be explained later in the section of controller design Eq. (16). The regulation mode selection is shown in Table 2, where ε is a small preset positive number.

OFF-SIDE PRESSURE REGULATOR DESIGN

The objective of the off-side pressure regulator is to keep the off-side pressure at a constant low pressure P_0. To illustrate the design procedure, this section designs a pressure regulator for those working modes, for which P_2 is the off-side. The regulator design for P_1 follows the same procedure and is omitted here.

The dynamics of P_2 is described in (3) and (4). In order to use parameter adaptation to reduce parametric uncertainties to improve performance, it is neccesary to linearly parameterize the system dynamics in terms of a set of unknown parameters θ_p. θ_p is defined as $\theta_p = [\theta_\beta, \theta_Q]^T$, where $\theta_\beta = \beta_e$ and $\theta_Q = \beta_e \tilde{Q}_{2n}$, $\tilde{Q}_{2n}$ is the nominal value of $\tilde{Q}_2$, i.e. $\tilde{Q}_2 = \tilde{Q}_{2n} + \Delta_Q$. The P_2 dynamics can be rewritten as follows.

$$\dot{P}_2 = \frac{A_2}{V_2}\frac{\partial x_L}{\partial q_2}\dot{q}_2\theta_\beta - \frac{\theta_\beta}{V_2}Q_{2M} - \frac{\theta_Q}{V_2} + \Delta_Q \tag{8}$$

The goal is to have the cylinder pressure regulated to a desired constant low pressure P_0. It is practical to assume that the parameters and Δ_Q are bounded by some known bounds, because both bulk modulus β_e and the modelling error of the flow mapping are practically bounded and the bound can be found with *a priori* information.

Define the pressure regulation error as $e_{p2} = P_2 - P_0$, the error dynamics would be same as the pressure dynamics because P_0 is constant.

$$\dot{e}_{P2} = -\frac{\theta_\beta}{V_2}Q_{2M} + \frac{A_2}{V_2}\frac{\partial x_L}{\partial q_2}\dot{q}_2\theta_\beta - \frac{\theta_Q}{V_2} + \Delta_Q \tag{9}$$

Q_{2M} is the control input and the control law can be defined as:

$$Q_{2M} = (k_{p2} + k_{p2s})\frac{V_2}{\theta_{\beta min}}e_{p2} + A_2\frac{\partial x_L}{\partial q_2}\dot{q}_2 - \frac{\hat{\theta}_Q}{\hat{\theta}_\beta} \tag{10}$$

where $(A_2\frac{\partial x_L}{\partial q_2}\dot{q}_2 - \frac{\hat{\theta}_Q}{\hat{\theta}_\beta})$ is the model compensation term and called as Q_{2Ma}, $k_{p2} > 0$, and $k_{p2s}\frac{V_2}{\theta_{\beta min}}e_{p2}$ is the robust term to dominate the parameter estimation error and unmodelled disturbances, which is chosen to satisfy the following conditions:

$$e_{p2}(k_{p2s}\frac{\theta_\beta}{\theta_{\beta min}}e_{p2} - \phi_{p2}^T\tilde{\theta}_{p2} + \Delta_Q) \geq 0$$
$$k_{p2s} \geq 0 \tag{11}$$

Copyright © 2003 by ASME

The parameter adaptation law is defined as

$$\dot{\hat{\theta}}_p = Proj_{\theta_p}(\Gamma_p \phi_{p2} e_{p2}) \tag{12}$$

where Γ_p is positive definite diagonal adaptation rate matrix, and $\phi_{p2} = [\frac{A_2}{V_2}\frac{\partial x_L}{\partial q_2}\dot{q}_2 - \frac{Q_{2Ma}}{V_2}, \quad -\frac{1}{V_2}]^T$.

The above adaptive robust control law (10) and adaptation law (12) provides prescribed transient response and final tracking accuracy in general and asymptotic tracking in the absence of uncertain disturbance. Theoretical proof of standard ARC performance can be found in [15–17].

ADAPTIVE ROBUST MOTION CONTROLLER DESIGN

The dynamics of the boom motion and pressures at both chambers are described in (2) and (3). Define a set of parameters as $\theta = [\theta_1, ..., \theta_6]^T$, $\theta_1 = \frac{1}{1+\frac{l_e^2}{J_c}m_L}$, $\theta_2 = \frac{D_f}{J_c + m_l l_e^2}$, $\theta_3 = \frac{T_n}{J_c + m_L l_e^2}$, $\theta_4 = \beta_e$, $\beta_e \tilde{Q}_{1n}$, $\theta_7 = \beta_e \tilde{Q}_{2n}$. It is practically to assume that all parameters and disturbances are bounded and the bounds can be estimated with *a priori* information.

The system dynamics equations can be rewritten as:

$$\begin{aligned}
\ddot{q}_2 &= \frac{\theta_1}{J_c}\left[\frac{\partial x_L}{\partial q_2}(P_1A_1 - P_2A_2) - G_c\right] \\
&\quad + \frac{\theta_1}{l_e^2} g l_g - \dot{q}_2\theta_2 + \theta_3 - \frac{1}{l_e^2} g l_g + \Delta \\
\dot{P}_1 &= -\frac{A_1}{V_1}\frac{\partial x_L}{\partial q_2}\dot{q}_2\theta_4 + \frac{\theta_4}{V_1}Q_{1M} + \frac{\theta_5}{V_1} + \Delta_{Q_1} \\
\dot{P}_2 &= \frac{A_2}{V_2}\frac{\partial x_L}{\partial q_2}\dot{q}_2\theta_4 - \frac{\theta_4}{V_2}Q_{2M} - \frac{\theta_6}{V_2} + \Delta_{Q_2}
\end{aligned} \tag{13}$$

To illustrate the adaptive robust motion controller design, this section presents a design procedure for those working modes, whose working side is the head end chamber, i.e. P_1. The controller design for P_2 follows the same procedure and is omitted here.

Step 1

Define a switching-function-like quantity as

$$z_2 = \dot{z}_1 + k_1 z_1 = \dot{q}_2 - \dot{q}_{2r}, \quad \dot{q}_{2r} \triangleq \dot{q}_{2d} - k_1 z_1 \tag{14}$$

where $z_1 = q_2 - q_{2d}(t)$ is the output tracking error with $q_{2d}(t)$ being the reference trajectory. Differentiate (14) while noting (13)

$$\dot{z}_2 = \theta_1\left[\tfrac{1}{J_c}(\tfrac{\partial x_L}{\partial q_2}P_L - G_c) + \tfrac{1}{l_e^2} g l_g\right] - \tfrac{1}{l_e^2} g l_g - \ddot{q}_{2r} - \theta_2\dot{q}_2 + \theta_3 + \Delta \tag{15}$$

where $P_L = P_1A_1 - P_2A_2$ is defined as the load force. If we treat P_L as the control input to (15), we can synthesize a virtual control law P_{Ld} such that z_2 is as small as possible. Since (15) has both parametric uncertainties θ_1 through θ_3 and uncertain nonlinearity Δ, the ARC approach proposed by Yao [15] will be generalized to accomplish this system.

The design details are similar to those in [5, 6] and omitted. The resulting control function P_{Ld} consists of two parts given by

$$\begin{aligned}
&P_{Ld}(q_2, \dot{q}_2, \hat{\theta}_1, \hat{\theta}_2, t) = P_{Lda} + P_{Lds} \\
&P_{Lda} = \tfrac{\partial q_2}{\partial x_L}\left[G_c + \tfrac{J_c}{\hat{\theta}_1}(-\tfrac{\hat{\theta}_1}{l_e^2} g l_g + \hat{\theta}_2\dot{q}_2 - \theta_3 + \tfrac{1}{l_e^2} g l_g + \ddot{q}_{2r})\right] \\
&P_{Lds} = P_{Lds1} + P_{Lds2}, \;\; P_{Lds1} = -\tfrac{J_c}{\theta_{1min}}\tfrac{\partial q_2}{\partial x_L}k_2 z_2
\end{aligned} \tag{16}$$

in which P_{Lda} functions as an adaptive model compensation, and P_{Lds} is a robust control law with $k_2 > 0$, and P_{Lds2} is chosen to satisfy the following robust performance conditions as in [5]

$$\begin{aligned}
&\text{i} \qquad z_2[\tfrac{1}{J_c}\theta_1\tfrac{\partial x_L}{\partial q_2}P_{Lds2} - \tilde{\theta}^T\phi_2 + \Delta] \le \varepsilon_2 \\
&\text{ii} \qquad z_2\tfrac{\partial x_L}{\partial q_2}P_{Lds2} \le 0
\end{aligned} \tag{17}$$

where ε_2 is a design parameter. If P_L were the actual control input, the adaptation function as defined in [6] would be

$$\tau_2 = w_2\phi_2 z_2, \quad \phi_2 \triangleq \left[\tfrac{1}{J_c}(\tfrac{\partial x_L}{\partial q_2}P_{Lda} - G_c) + \tfrac{1}{l_e^2} g l_g, -\dot{q}_2, 1, 0, 0, 0\right]^T \tag{18}$$

where $w_2 > 0$ is a constant weighting factor.

Step 2

Let $z_3 = P_L - P_{Ld}$ denote the input discrepancy. In this step, a virtual control flow will be synthesized so that z_3 converges to zero or a small value with a guaranteed transient performance and accuracy.

From (13),

$$\begin{aligned}
\dot{z_3} &= \dot{P}_L - \dot{P}_{Ld} \\
&= -\left(\tfrac{A_1^2}{V_1} + \tfrac{A_2^2}{V_2}\right)\tfrac{\partial x_L}{\partial q_2}\dot{(q)}_2\theta_4 + \tfrac{A_2}{V_2}\theta_4 Q_{2M} + \tfrac{A_1}{V_1}\theta_5 + \tfrac{A_2}{V_2}\theta_6 \\
&\quad -\dot{P}_{Ldc} + \tfrac{A_1}{V_1}\theta_4 Q_{1M} + A_1\Delta_{Q1} - A_2\Delta_{Q2} - \dot{P}_{Ldu}
\end{aligned} \tag{19}$$

where

$$\begin{aligned}
&\dot{P}_{Ldc} = \tfrac{\partial P_{Ld}}{\partial q_2}\dot{q}_2 + \tfrac{\partial P_{Ld}}{\partial \dot{q}_2}\dot{\hat{q}}_2 + \tfrac{\partial P_{Ld}}{\partial t} \\
&\dot{P}_{Ldu} = \tfrac{\partial P_{Ld}}{\partial \dot{q}_2}[-\tfrac{\tilde{\theta}_1}{J_c}(\tfrac{\partial x_L}{\partial q_2}P_L - G_c) - \tfrac{\tilde{\theta}_1}{l_e^2} g l_g(q_2) + \tilde{\theta}_2\dot{q}_2 - \tilde{\theta}_3 + \Delta] + \tfrac{\partial P_{Ld}}{\partial \hat{\theta}}\dot{\hat{\theta}}
\end{aligned} \tag{20}$$

in which $\hat{\dot{q}}_2$ represent the calculable part of $\ddot{q}_2$ given by

$$\hat{\dot{q}}_2 = \tfrac{\hat{\theta}_1}{J_c}[\tfrac{\partial x_L}{\partial q_2}P_L - G_c] + \tfrac{\hat{\theta}_1}{l_e^2} g l_g - \hat{\theta}_2\dot{q}_2 + \hat{\theta}_3 - \tfrac{1}{l_e^2} g l_g \tag{21}$$

Copyright © 2003 by ASME

In (20), $\dot{P}_{Ldc}$ is calculable and can be used in the construction of control functions, but $\dot{P}_{Ldu}$ cannot due to various uncertainties. Therefore, $\dot{P}_{Ldu}$ has to be dealt with via certain robust feedback in this step design.

In viewing (19), Q_{1M} can be thought as the control input for (19) and step 2 is to synthesize a control function Q_{1Md} for Q_{1M} such that P_L tracks the desired control function P_{Ld} synthesized in Step 1 with a guaranteed transient performance.

Similar to (16), the control function Q_{1Md} consists of two parts given by

$$\begin{aligned} &Q_{1Md}(q_2,\dot{q}_2,P_1,P_2,\hat{\theta},t) = Q_{1Mda} + Q_{1Mds} \\ &Q_{1Mda} = \frac{V_1}{A_1\hat{\theta}_4}[-\frac{\hat{\theta}_1}{J_c}\frac{\partial x_L}{\partial q_2}z_2 + \hat{\theta}_4\left((\frac{A_1^2}{V_1}+\frac{A_2^2}{V_2})\frac{\partial x_l}{\partial q_2}\dot{q}_2 - \frac{A_2}{V_2}Q_{2M}\right) \\ &\qquad -\hat{\theta}_5\frac{A_1}{V_1} - \hat{\theta}_6\frac{A_2}{V_2} + \dot{P}_{Ldc}] \\ &Q_{1Mds} = Q_{1Mds1} + Q_{1Mds2},\ \ Q_{1Mds1} = -\frac{V_1}{A_1\theta_{4min}}k_3 z_3 \end{aligned} \tag{22}$$

where $k_3 > 0$.

Like (17), Q_{1Mds2} is a robust control function chosen to satisfy the following two robust performance conditions

$$\begin{aligned} &\text{i} \qquad z_3\left[\theta_4 Q_{1Mds2} - \tilde{\theta}^T\phi_3 - \frac{\partial P_{Ld}}{\partial \dot{q}_2}\Delta + A_1\Delta_{Q_1} - A_2\Delta_{Q_2}\right] \le \varepsilon_3 \\ &\text{ii} \qquad z_3 Q_{1Mds2} \le 0 \end{aligned} \tag{23}$$

where ε_3 is a positive design parameter. The adaptation function as defined in [] would be

$$\tau = \tau 2 + \phi_3 z_3 \tag{24}$$

where ϕ_3 is defined as:

$$\phi_3 \triangleq \begin{bmatrix} \frac{1}{J_c}\frac{\partial x_L}{\partial q_2}z_2 - \frac{\partial P_{Ld}}{\partial \dot{q}_2}[\frac{1}{J_c}(\frac{\partial x_L}{\partial q_2}P_L - G_c) + \frac{1}{l_e^2}gl_g] \\ \frac{\partial P_{Ld}}{\partial \dot{q}_2}\dot{q}_2 \\ -\frac{\partial P_{Ld}}{\partial \dot{q}_2} \\ -\left(\frac{A_1^2}{V_1}+\frac{A_2^2}{V_2}\right)\frac{\partial x_L}{\partial q_2}\dot{q}_2 + \frac{A_2}{V_2}Q_{2M} + \frac{A_1}{V_1}Q_{1Ma} \\ \frac{A_1}{V_1} \\ \frac{A_2}{V_2} \end{bmatrix} \tag{25}$$

With the above ARC controller, it can be proven that the same theoretical motion tracking performance results as in [5, 6] are obtained. The details are omitted.

Once the control functions Q_{1Md} for Q_{1M} is synthesized as given in (22), the next step is to use the pressure compensated inverse valve mappings to calculate the specific valve control voltage command to provide the desired "flows"— Q_{1Md}. The details can be worked out easily and are omitted.

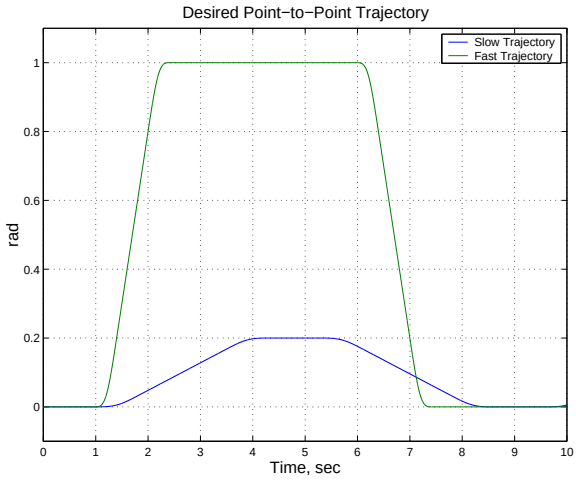

Figure 3. POINT-TO-POINT DESIRED TRAJECTORIES.

SIMULATION AND EXPERIMENTS

Some simplifications have been made when implementing the proposed control strategy. The selection of the specific robust control terms by (11), (17) and (23) is rigorous and should be the formal approach to choose. However, it increases the complexity of the resulting control law considerably since it may need significant amount of computation time to calculate the lower bounds. As an alternative, a pragmatic approach is to simply choose k_{p2}, k_2 and k_3 large enough without worrying about the specific values of k_{p2s}, k_{2s} and k_{3s}. By doing so, (11), (17) and (23) will be satisfied at least locally around the desired trajectory. On the one hand, we hope all the gains are as large as possible to have faster response and stronger ability to reject disturbance; on the other hand, too large gains (high bandwidth) may excite the unmodelled dynamics and cause instability. For this system, because we neglected the valve dynamics which is about $353 rad/sec$, it is safer to keep the closed loop bandwidth less than $35 rad/sec$, which is a guideline to choose gains.

The complete controller is simulated in Simulink. The ARC motion controller parameters used in simulations are: $k_1 = k_2 = k_3 = 35$, $\Gamma = diag\{1e-11,\quad 1e-10,\quad 2e-8,\quad 8e+4,\quad 1e-4,\quad 1e-4\}$. The parameters for the off-side pressure regulator are: $k_p = 35$ and $\Gamma_p = diag\{2e+4,\quad 1e-6\}$. The desired constant low pressure for off-side is $P_0 = 200KPa$. The controller is tested for two point-to-point trajectories, shown in figure 3. The fast trajectory has maximal angular acceleration and velocity as $5 rad/s^2$ and $1 rad/s$, which is close to the physical limit; the slow trajectory $0.2 rad/s^2$ and $0.08 rad/s$.

The simulation results with and without a $25Kg$ load are shown in Fig. 4 through Fig. 7, where first plot represents tracking error, second represents angular velocity, third one are the pressures at the two chambers, fourth one shows the energy usage of this system and a system with load sensing pump, the last

Copyright © 2003 by ASME

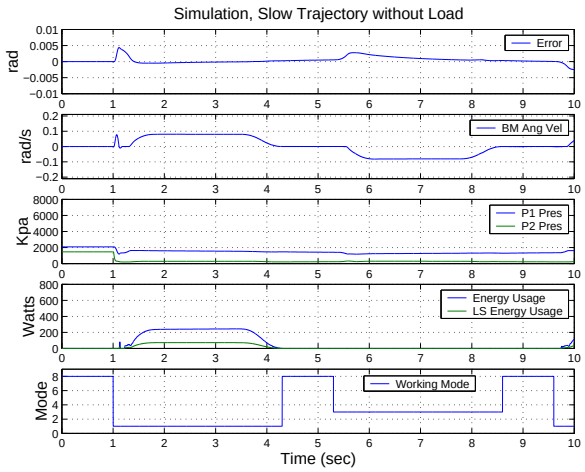

Figure 4. SIMULATION, SLOW TRAJECTORY WITHOUT LOAD.

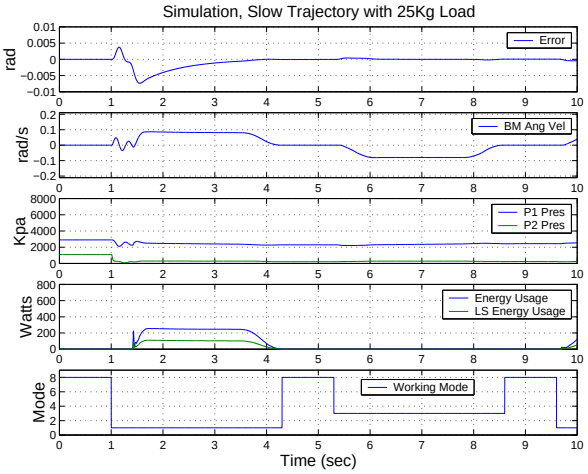

Figure 5. SIMULATION, SLOW TRAJECTORY WITH 25Kg LOAD.

one represents the selected working mode (1—5 represent tracking mode T1-T5, 6—8 regulation mode R1-R3). The simulations show that the controller performs very well in each case with a maximum error less than 0.01*rad* and the final tracking accuracy down to resolution level. The cylinder pressures in both cases remain very low, thus increasing efficiency of the system. The energy usage is calculated as the pump flow times the pressure drop from pump to tank. The energy usage is zero when the cylinder is working in tracking mode T3 or regulation modes R1 or R3, because regeneration flow is used to power the cylinder motion. The zero energy consumption can be observed in the period from 5 to 9 seconds. The plot of the energy usage includes an additional line representing the potential decrease in energy usage with a load sensing pump. The current set up and simulation makes use of a constant pressure supply that is not highly efficient. A load sensing pump that can provide the needed flow at the highest working pressure would significantly reduce the energy usage if used in conjunction with the programmable valve. The plot labelled as 'LS Energy Usage' calculates the anticipated energy usage if a load sensing pump was used. It also assumes that the pump would track the highest working pressure and add an additional 500*KPa* margin of pressure.

The completed controller is also implemented on the hydraulic system and tested identically to the tests run in the simulation results. In the actual implementation of the controller a number of changes are necessary. Due to limited bandwidth of the valve the controller gains are lowered from 35 to 20 to reduce control signal chattering.

The experimental results with and without a 25*Kg* load, Fig. 8 through Fig. 11, show that the controller performs well in each case with a maximum error less then 0.02*rad*. The difference between the simulation and experimental results is the differing gains used. The cylinder pressures in both cases remain very low,

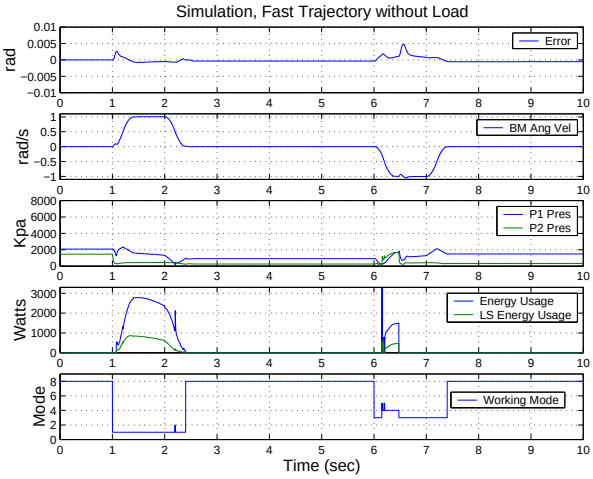

Figure 6. SIMULATION, FAST TRAJECTORY WITHOUT LOAD.

thus reducing energy usage of the system. The energy usage is calculated as the pump flow times the pressure drop from pump to tank. The energy usage is zero when the cylinder is working in tracking mode T3 and regulation modes R1 and R3, when regeneration flow is used, as seen between the time of 5-9 seconds. The plot of the energy usage includes an additional line representing the potential decrease in energy usage with a load sensing pump as seen in the simulation results.

CONCLUSIONS

The coordinate control of energy-saving programmable valves presented in this paper achieves excellent tracking performance and significant reduction of energy usage. The dual objectives of good tracking and energy-saving are made possible

Copyright © 2003 by ASME

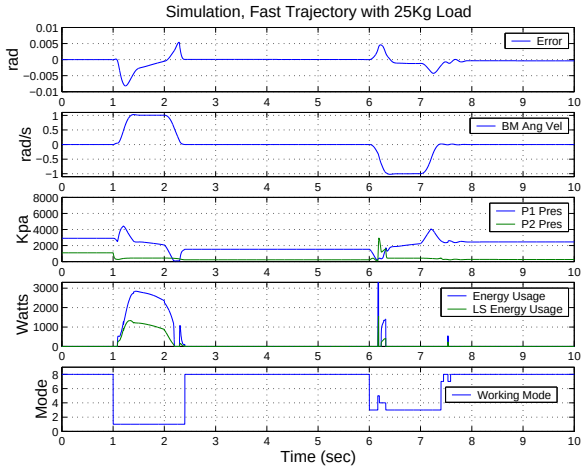

Figure 7. SIMULATION, FAST TRAJECTORY WITH 25Kg LOAD.

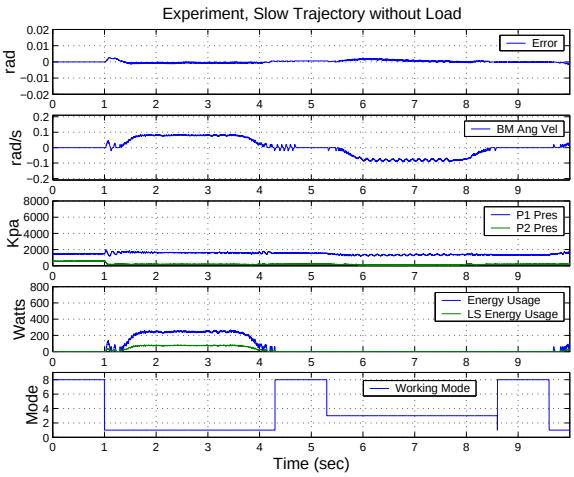

Figure 8. EXPERIMENT, SLOW TRAJECTORY WITHOUT LOAD.

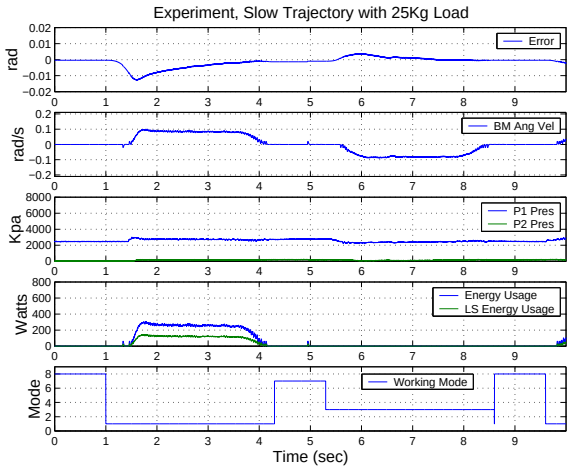

Figure 9. EXPERIMENT, SLOW TRAJECTORY WITH 25Kg LOAD.

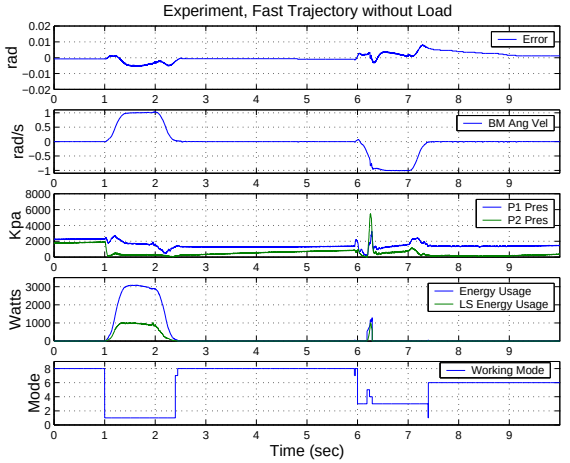

Figure 10. EXPERIMENT, FAST TRAJECTORY WITHOUT LOAD.

by the flexible programmable valve system. The adaptive robust control technique guarantees prescribed tracking performance even in the presence of unmodelled uncertainties and external disturbances. And incorporating the off-side dynamics into the controller design further increase the system performance. Both simulations and experiments show very small tracking errors in the transient period, almost asymptotic tracking, smooth mode changing and almost constant off-side pressure. The experiment results also show that the final tracking accuracy is down to the resolution level.

REFERENCES

[1] Merritt, H. E., 1967. *Hydraulic Control Systems*. John Wiley & Sons.

[2] Tsao, T., and Tomizuka, M., 1994. "Robust adaptive and repetitive digital control and application to hydraulic servo for noncircular machining". *ASME J. Dynamic Systems, Measurement, and Control*, **116**, pp. 24–32.

[3] FitzSimons, P., and Palazzolo, J., 1996. "Part i: Modeling of a one-degree-of-freedom active hydraulic mount; part ii: Control". ASME J. Dynamic Systems, Measurement, and Control, **118** (4), pp. 439–448.

[4] Plummer, A., and Vaughan, N., 1996. "Robust adaptive control for hydraulic servosystems". *ASME J. Dynamic Systems, Measurement, and Control*, **118**, pp. 237–244.

[5] Yao, B., Bu, F., Reedy, J. T., and Chiu, G. T., 2000. "Adaptive robust control of singal-rod hydraulic actuators: Theory and experiments". The IEEE/ASME Trans. on Mecha-

Copyright © 2003 by ASME

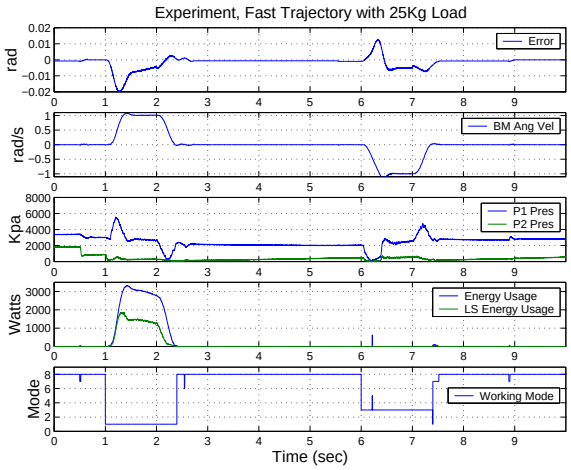

Figure 11. EXPERIMENT, FAST TRAJECTORY WITH 25Kg LOAD.

tronics, **5** (1), pp. 79–91.

[6] Bu, F., and Yao, B., 2000. "Nonlinear adaptive robust control of hydraulic actuators regulated by proportional directional control valves with deadband and nonlinear flow gain coefficients". In Proc. of American Control Conference, pp. 4129–4133.

[7] Bu, F., and Yao, B., 1999. "Adaptive robust precision motion control of singal-rod hydraulic actuatorswith timevaring unknown inertia: A case study". In ASME International Mechanical Engineering Congress and Exposition (IMECE'97), vol. FPST-6, pp. 131–138.

[8] Jansson, A., and Palmberg, J.-O., 1990. "Seperate control of meter-in and meter-outorifices in mobile hydraulic systems". ASE Transactions, **99** (2), pp. 337–383.

[9] Kramer, K., and Fletcher, E., 1990. "Electrohydraulic valve system". *United States Patent, Re. 33,846*.

[10] Garnjost, K., 1989. "Energy-conserving regenerative-flow valves for hydraulic servomotors". *United States Patent, 4,840,111*.

[11] Aardema, J., and Koehler, D., 1999. "System and method for controlling an independent metering valve". *United States Patent, 5,947,140*.

[12] Book, R., and Goering, C., 1999. "Programmable electrohydraulic valve". ASE Transactions, **108** (2), pp. 346–352.

[13] Watton, J., 1989. *Fluid Power Systems*. Prentice Hall.

[14] Liu, S., and Yao, B., 2002. "Energy-saving control of single-rod hydraulic cylinders with programmable valves and improved working mode selection". In IFEPE/SAE'02.

[15] Yao, B., 1997. "High performance adaptive robust control of nonlinear systems: a general framework and new schemes". In Proc. of IEEE Conference on Decision and Control, pp. 2489–2494.

[16] Yao, B., and Tomizuka, M., 1997. "Adaptive robust control of siso nonlinear systems in a semi-strict feedback form". Automatica, **33** (5), pp. 893–900.

[17] Yao, B., and Tomizuka, M., 2001. "Adaptive robust control of mimo nonlinear systems in a semi-strict feedback form". Automatica, **37** (9), pp. 1305–1321.

Copyright © 2003 by ASME